Methods for improving the stability of perovskite materials and their conversion efficiency

Zhuoxuan Li[1,*], Lingfei Yin[2] and Xiaoxi Zong[3]

[1] School of Chemistry and Materials Science, Nanjing University of Information Science & Technology, Nanjing, 210044, China
[2] The Leicester International Institute, Dalian University of Technology, Dalian, 323900, China
[3] School of Chemistry and Chemical Engineering, Shaoxing University, Shaoxing, 312000, China

[*] 201913380036@nuist.edu.com

Abstract. The research on perovskite thin film solar cells has made great progress in recent years and is believed to be a material with enormous potential for development. However, problems like relatively poor stability, environmental unfriendliness and low large-area photoelectric conversion efficiency remain to solve. Its large-scale production is still a long way off. This study introduces the recent progress of the perovskite materials for perovskite solar cells and reviews the three ways of improving the stability and photoelectric conversion efficiency of perovskite materials for solar cells, including dye sensitization, doping and graphene oxidation. Diverse dyes for sensitization of perovskite materials are listed, and their mechanics are briefly introduced. The principles of how doping and graphene oxidation improve the stability and photoelectric conversion efficiency of perovskite materials are also described in this manuscript. Finally, based on those methods, suggestions for the future development of perovskite materials for solar cells are provided.

Keywords: perovskite material, solar cell, conversion efficiency, stability.

1. Introduction

The third generation of solar cells, known as perovskite solar cells (PSCs), use perovskite-type organometallic compound transistors as solar-absorbing components to convert light energy directly into electricity via the photoelectric effect. In 2009, Miyasaka et al. first applied the material of calcium titanite structure to dye-sensitized solar cells and obtained the calcium titanite solar cells with a 3.8% approximate efficiency of photoelectric conversion [1]. Hybrid perovskite solar cells have recently gained much attention because of their affordability, adaptability, and high performance. Although these cells have high photoelectric conversion efficiency, their chemical properties are unstable. On the road to practical applications of perovskite solar cells, Two things must be prioritized: one is the photoelectric conversion efficiency, and the other is the device stability [2-4].

Here is a brief description of the usual laboratory preparation of perovskite in four steps. The titanium dioxide film is first prepared on the FTO glass by sintering at 45 °C, after which a precursor solution containing CH_3NH_3I is dropped on the titanium dioxide, and the final film of perovskite structure is formed by sintering at 90 °C. Care should be taken to close it with a sealing film. Otherwise, there is a risk of decomposition [5].

Current perovskites are ionic crystals, and their common constituents [iodide ions (I^-), lead ions (Pb^+), and methylamine ions (ma^+)] are prone to polarization reactions by combining with oxygen and water molecules in the air during the preparation process and device service, which affect the loss of photoelectric conversion efficiency and stability of the cell. In order to study the preparation of perovskite cells, the failure principle of perovskite is briefly introduced here. During the preparation of calcium titanite cells, the ambient conditions, such as water and oxygen, will directly affect the stability of the reaction 3-related components. Firstly, CH_3NH_3I is an extremely sensitive material to water, and it is easily hydrolyzed by water, making reaction 3 proceed to the left. When oxygen/UV light and water are present, CH_3NH_3I undergoes a series of reactions as followings:

$$\mathrm{PbI_2(s) + CH_3NH_3I(aq) \leftrightarrow CH_3NH_3PbI_3(s)} \tag{1}$$

$$\mathrm{CH_3NH_3I(aq) \leftrightarrow CH_3NH_2(aq) + HI(aq)} \tag{2}$$

$$\mathrm{4HI(aq) + O_2(g) \rightarrow 2I_2(s) + 2H_2O(l)} \tag{3}$$

$$\mathrm{2HI(aq) \xrightarrow{UV} H_2(g) + I_2(s)} \tag{4}$$

Furthermore, the decomposition of CH_3NH_3I causes the decomposition of perovskite, which makes the cell fail, as shown in Figure 1.

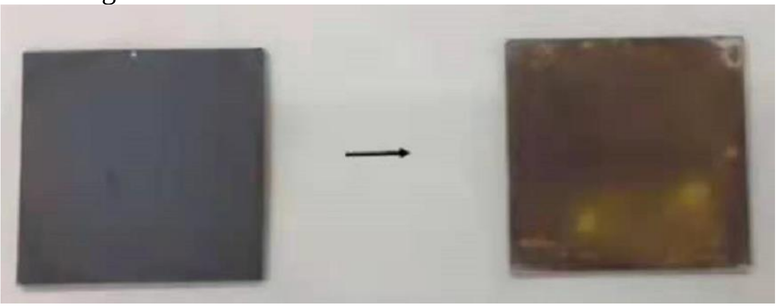

Figure 1. Chalcocite before and after failure.

On this basis, this paper summarizes three methods to improve the stability and photovoltaic conversion efficiency. The first approach combines dye-sensitized solar cells (DSSC) to solve the problem. DSSC has become an important research topic in the past two decades due to its importance in energy conversion. The redox coupling in the electrolyte then regenerates the molecule, and finally, the electrons migrate through the external load to complete the circuit. Complexes based on ruthenium are thought to be the most effective at creating 10–11% efficient DSSCs. However, because ruthenium is a precious metal that is expensive and rare, research on organic photosensitizers and natural dyes is essential to obtaining less expensive colors for DSSC. [6]. Current research shows that ruthenium-free dyes also have good photoelectric conversion efficiency, which suggests that they are promising photosensitizers for DSSC [7-9]. The second approach is to perform doping. Doping is often used in practice to improve certain properties of semiconductor materials. The use of doping in the study of perovskite solar cells can effectively improve the performance of each film layer material, thus ensuring the stability of perovskite cells. The third approach is to use GRMs in the form of graphene oxide (graphene oxide or reduced graphene oxide) as dopants and interlayers to enhance charge injection to the electrodes because of their versatility and ability to modify the edges and chemically functionalize them to manage the energy band gap and band alignment. In addition, they are beneficial to improve the device's lifetime under different stress conditions.

2. Combined dye-sensitized solar cells (DSSC)

Combining dye sensitizers in calcium titanite cells can effectively improve the stability and photoelectric conversion efficiency of calcium titanite cells. Here, several commonly used dyes for calcium titanite cells are introduced.

2.1. Ru-complex dyes

Due to the octahedral shape of their Ru (II) complexes, which have adjustable photophysical, photochemical, and chemical stability, Ru-based DSSCs have achieved exceptional success. It also exhibits strong solubility in various solvents and stable, reachable oxidation levels from I to IV. Although expensive, organic photosensitizers and natural dyes are crucial to obtaining less expensive dyes for DSSC [10].

2.2. Coumarin

Coumarin, molecular formula $C_9H_6O_2$, white crystalline solid, exists in black coumarin, coumarin, wild coumarin, and orchid, with fresh hay and coumarin fragrance not for consumption, allowing for smoke and external use. Taking the first coumarin, C343, as an example, the conversion efficiency of this particular compound was found to be low due to the narrow absorption spectrum of C343. Adding more methane groups contributes to the extension of the π-conjugate linker and thus helps improve the efficiency of DSSC [11].

2.3. 3,4,9,10-tetracarboxylic dianhydride PTCDA

Figure 2 gives the two ways of preparation of a calcium titanite cell combined with this dye. First, the sintered titanium dioxide is prepared, after which the dye is attached to it for one day, after which the precursor solution is added dropwise and sintered at 90 °C to form a calcium titanate film. Thus, the dye is formed in the internal state. Moreover, the other way is to prepare the calixarene film first and then drip the dye on the surface, thus forming the dye on the outside.

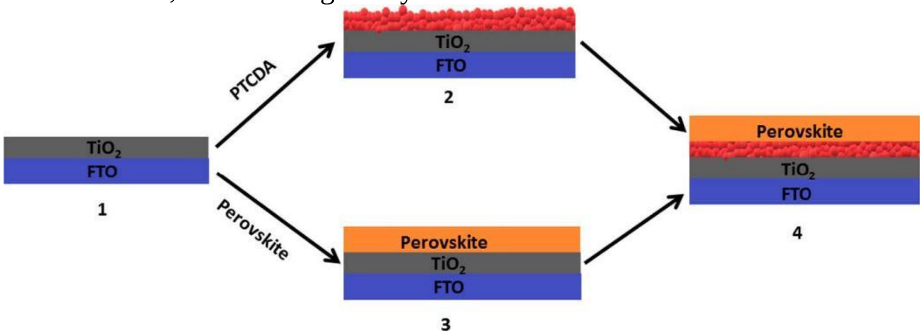

Figure 2. Principle demonstration of the two ways of preparing a calcium titanite cell combined with dye, 1 – 4 represents (1) the FTO's bare TiO_2 film and the perylene dye molecules (red dots), (2) the TiO_2 film using bare PTCDA sensitized, (3) the halide perovskite layer film, (4) and the combination film of perovskite, dye and TiO_2 [5].

When exposed to visible light, the dye/calcite systems 1 to 4 dissolved in water yield a range of photocurrent values (Figure 3a), with the dye-sensitized calcium titanite system exhibiting the highest photovoltaic performance. For instance, compared to 3, 4 generates twice as much water-based photocurrent. The TiO_2 and dye-sensitized TiO_2 systems in systems 1 and 2 responded only to UV and near-UV light, with unimpressive light absorption and charge transfer performance. The systems based on TiO_2 1 and 2 without a chalcogenide layer produced minimal photocurrents. Conversely, when 3 contains a halide chalcogenide capping layer, the equivalent photocurrent value rises instantly when the visible light is turned on within the first 20 seconds, exceeding 3 $\mu A/cm^2$, which is a factor of two greater than 3 and 2. According to this study, the halide chalcogenide layer induces a noticeably updated visible light, which encourages electronic conductivity between the photoanode and the neighboring substrate or electrolyte. Finally, the photocurrent value decreased to 3 $\mu A/cm^2$. After 20 seconds of illumination, this was attributed to the halide chalcogenide material's water solubility. At 200 s, the photocurrent stabilized at 2.5 μA/cm^2.

Compared to other systems, the chalcogenide and TiO_2 system's addition of perylene dyes considerably improved the photocurrent generation. The dye/calcium titanite photoanode 4 demonstrated a photocurrent of 8 μA/cm^2 when the dye based on perylene was present, twice the photocurrent produced by 3. The chalcogenide system 4, based on perylene dye, has solubility and instability issues in aqueous solutions. As an illustration, 4 generated a photocurrent of 5 μA/cm^2 after 190 s, which is around 60% of the initial amount. The inflexible structural systems of the perylene-based system and the susceptibility of the halide chalcogenide material to aqueous dyes, which inhibited rotation of the molecules and resulted in lower adsorption, are blamed for the chemical reaction of the perylene-based dye-sensitized chalcogenide system. However, after 200 s, the dye-sensitized chalcogenide system instantly produced a photocurrent lower than 10 μA/cm^2, which was a much higher photocurrent generation than the other systems. System 4 produces the biggest photocurrent in the solution with water, and the photocurrent generation in an aqueous solution quantifies the photoelectric characteristics in the order of 4 > 3, and the 1 and 2 have a similar range.

The I-V parameters of 1-4 further highlight the enhanced photocurrent capability of the dye-sensitized perylene chalcogenide deceive (Figure 3b). The four systems' I-V curves are in the following decreasing order. For instance, 4 at no voltage has a photocurrent value more than 1-3: At 20 s, 4 has a photocurrent of 46 A, 3 has a photocurrent of 6 A at the same time, and 1 and 2 have a photocurrent of 2 A. As a result, while the photocurrent between 1 and 2 is slightly different from 3, it is significantly bigger than 1 to 2. This highlights how the dye-sensitization technique can be used to enhance the halide chalcogenide films' water-based photovoltaic characteristics.

The I-V and photocurrent curves exhibit a similar pattern to the 1-4 UV-Vis absorption spectrum (Figure 3c). For instance, sample 4 of the dye-sensitized carcinogens had the best light capture performance from highest to lowest UV-Vis absorption performance. The TiO_2 layer was exclusively reactive in the UV region in Sample 1, which displayed very little visible light taken. After adding the perylene dye layer, sample two can absorb maximum 500 nm wave, demonstrating that the added perylene dye, while sensitized, enhances the TiO_2 film's ability to absorb solar around 500 nm.

The dye sensitization stage further enhanced the bare chalcogenide/TiO_2 films' ability to trap light in cases 3 and 4, leading to a much higher short wavelength uptake efficiency between 400 and 600 nm for 4 than for 3. Additionally, the "1 + 1 > 2" effect suggested that the optical properties of the chalcogenide films and the perylene dioxide dye were improved synergistically, as in the visible zone, the combination of the intake capacity of 2 and 3 is much less than 4.

Overall, the perylene dye's excellent overall efficiency is based on the fact that it enhances the halide perovskite film's ability to trap light in the visible range and lowers charge complexation as in photoelectrode.

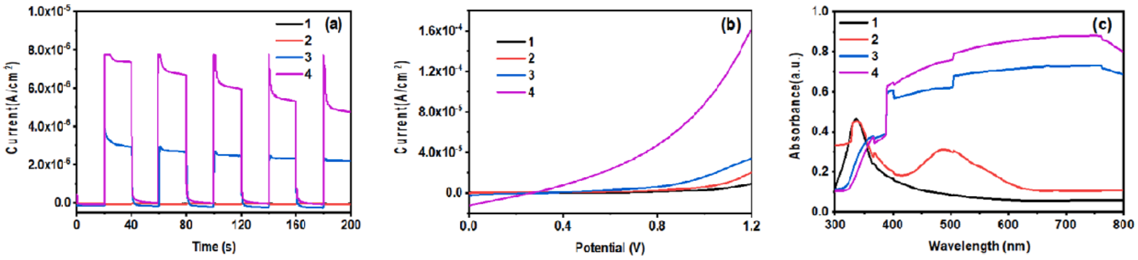

Figure 3. (a) Photocurrents 1–4 in the water-based formulation. (b) 1–4 curves I-V. (c) 1-4's UV-vis absorption spectrum. Ag/AgCl is used to evaluate the voltage [5].

2.4. Rhodamine B

Rhodamine B, used as a photosensitizer, is a thousand times cheaper than ruthenium-based or other organic dyes. Figure 4 gives its molecular structure of it. The results of a cheap rhodamine B dye concentration on the performance of ZnO NP-based DSSC were investigated, and the photon-to-electricity transforming ability of DSSC was found to increase from 0.07% to 0.58%, an eight-fold increase. The results suggest that rhodamine B has a significant cost advantage in DCCS applications [12].

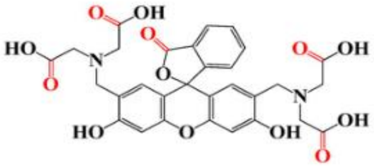

Figure 4. Molecular structure of rhodamine B [12].

2.5. Calixanthin

Chen, Zhang et al. showed that enhanced photovoltaic properties were obtained when the calixanthin dye was doped into the perovskite material. The structural formula of calixanthin is given in Figure 5. Under the same conditions, the photocurrent values generated by the photovoltaic electrodes composed of calcium xanthophyll\$CH_3NH_3PbI_3$ hybrid films were several orders of magnitude higher than those of bare CH_3NH_3 PbI_3 photovoltaics. The calcium xanthophyll dye improves the luminescence performance of $CH_3NH_3PbI_3$-based photoelectrodes in water, and calcium xanthophylls can make it more sensitive to light and passivate the calcium titanite electrodes. Therefore, calixanthin is also a better dye [13].

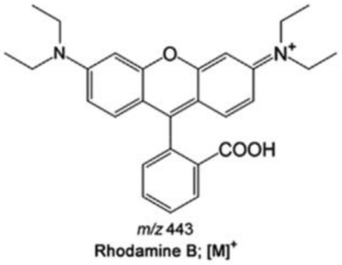

Figure 5. The structural formula of calixanthin [13].

3. Doping

In literature, doping small elements into structural lattice is commonly regarded as an effective approach to improve the performance of semiconductor materials, such as transition efficiency and the device's lifetime. Usually, submerged olive solar cells are mainly composed of a glass layer, electron transmission (ETM), perovskite layer, cave transmission layer (HTM) and metal electrodes covered with a transparent conductive film.

For a solar cell, the electron transport layer (ETL) function is designed to restrain the undesirable migration of electrons toward the cathode, resulting in an increased carrier extraction rate. Therefore, the ETL plays a crucial section in cutting-edge solar cells. Therefore, the electron transport layer is crucial in realizing PCSs devices. There are two main electron transport materials commonly used in perovskite solar cells: metal oxide and organic electron transport materials. TiO_2 and ZnO are the most common and most used electronic transport materials [14-18], and doping can improve electron mobility, thereby improving the device's overall efficiency.

The difference in elern migration rate increases the material of the TiO_2 ETL or effectively reduces the energy level between the ETL and the perovskite layer; Mixing ZnO electron transport layers can effectively improve the surface morphology of ZnO films. Reduce the composites of electronic caves. Graphene nanosheets offer excellent charge collection in nanocomposites based on the solution deposition method [16], using graphene and TiO_2 nanoparticle composites as light-absorbing layers. Nanoparticle composites are graphene doped with TiO_2 as the electron transport layer. Since the working function of graphene is located between the transparent FTO electrode and the TiO_2 electron transport layer, as shown in Figure 6(a) [16], the addition of graphene improves the efficiency of electron transfer, the short circuit current and filling factor of the device are significantly improved. This ultimately translates into efficiency of 15.6% for prepared perovskite solar cell devices. Under the light and dark conditions of AM1.5, the J-V curve of the device with only TiO_2 as the ETL, graphene as the electron transport layer, high-temperature sintered TiO_2 as the electron transport layer and no electron transport layer is simulated, as shown in Figure 6(b). The J-V curve of PSCs (η = 15.6%) of graphene-TiO_2 nanocomposites prepared under AM1.5 and dark light is shown in Figure 6. This proves that the doping of graphene can very well improve the capacity and stability of perovskite batteries.

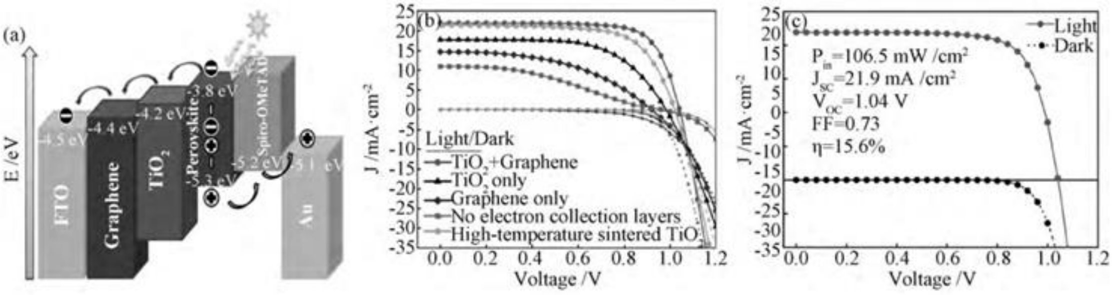

Figure 6. Doping position X of perovskite solar cells. (a)Energy level diagram of a material ; (b) Current-voltage curves of five electron collection layers of two different rays; (c) The greatest behavior (η = 15.6%) of graphene-TiO_2nanocomposites under two different rays [16].

Doping the yttrium element into TiO_2 can also improve the electron transport capability [17]. A layer of polyethoxyethyleneamine (PEIE) is inserted between TiO_2 and ITO for energy level matching. Then by dissolving-recrystallizing, the grown perovskite, the efficiency of the finally obtained planar heterojunction perovskite solar cell is as high as 19.3%. Figure 7(a) shows the carrier lifetime and transient voltage decay curves of the device in controlled humidity, and Figure 7(a) shows the carrier lifetime and instantaneous photovoltage decay curves of the device in controlled humidity and dry environment [17], this shows the difference in the life of the wearer under the two conditions is not significant, the performance of the device is more stable after doping. Figure 7(b) shows the transient decay curve of the photocurrent of the electron transport layers TiO_2 and Y-TiO_2, which shows that the photocurrent value of the Electron Transport Layer TiO_2 under doping Y is large; that is, the value of the light current in the Electron Transport Layer TiO_2 is large, the slower electron complex indicates that the electron transport performance of the Y-doped TiO_2 electron transport layer is better. Gratzel et al. were able to overnumber yttrium trichloride in TiO_2 synthesis, which also showed improvements in the short-circuit current of the perovskite solar cell devices they prepared [18].

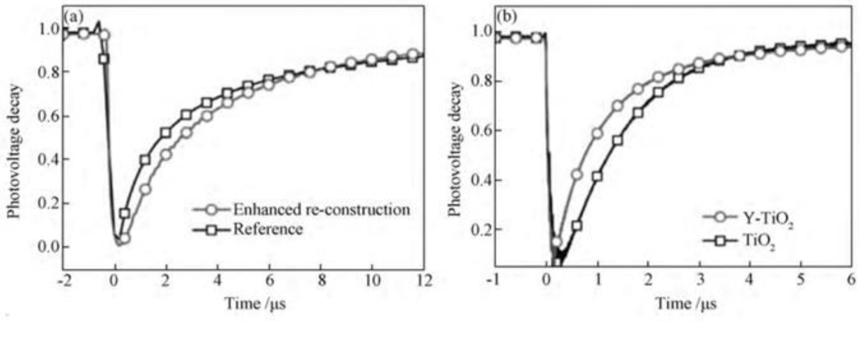

Figure 7. Transient photovoltage and transient photocurrent attenuation curves under different conditions. (a) Transient photo-voltage decay curves of devices in controlled humidity and dry air ;(b) Transient photocurrent decay curves of ETL devices of TiO_2 and Y-TiO_2 [17].

ZnO is also a commonly used electronic transport layer material. ZnO is a direct band gap semiconductor. Its electron mobility is higher than TiO_2, similar to TiO_2 [19,20]. It can be used as a hole block layer to block holes and prevent the composition of photonic carriers effectively. Through doping, the surface morphology of ZnO can be improved, thus effectively inhibiting the composition of photo carriers. Aluminum-doped ZnO (AZO) shells are introduced to ZnO nanoparticles as an electronic transmission layer for perovskite solar cells [21]. The efficacy of doped devices can be from 8.5% to 10.7%. Shirazi et al., using AZO as the electron transport layer and low-cost carbon as the electrode, explored the sexual energy of different aluminum doped (0% to 10%) devices under spray pyrolysis and showed that with the increase of aluminum doping from 0% to 5%, the filling of the device. The charging factor (FF), short-circuit current (J_{sc}), and photoelectric conversion efficiency (PCE) values gradually increase. However, when the amount of aluminum doping increased from 5% to 10%, these performance values began to decline again. After engineering optimization, the device efficiency reaches the optimal 8.23% when the dosage amount is 5%. The above study shows that doping improves perovskite cells' stability and photoelectric conversion efficiency [22].

4. Graphene and its derivatives

4.1. Mechanism

Though stability in the long term has become an issue, the increasing efficiency, high optical absorption, and high extent of flexibility make perovskite solar cells (PSCs) one of the most promising products in photovoltaic technology [22]. In the structure of the PSCs, the perovskite active layer generates electron-hole pairs during light absorption. After those pairs are separated, the electrons and holes enter the electron transport layer and hole transport layer (HTL). Transport materials with intrinsically exceptional properties will confer high quantum yield and the lifetime of the "electron-hole" pairs, thus extending the life of the battery and photoelectric conversion efficiency. Graphene and its derivatives acting as the interlayers or the dopant have been considered one of the effective methods to optimize the PSCs in both efficiency and stability [24]. In the structure of the graphene, one of the electrons on the 2S orbital undergoes an exciting transition into the 2Pz orbital and the other one altogether, with the electrons on the 2Px and 2Py orbitals forming three σ bonds via sp^2 hybridization; the Pz orbitals, perpendicular to the σ bonds and connected side by side, are bonded since the overlap of the electron clouds. These bonds are called π bonds, and they significantly contribute to the large mobility of the electrons, leading to excellent conductivity of the graphene materials. Moreover, the graphene oxide interface layer can contribute to the superior crystallization and orientation order of perovskite structure [26].

4.2. Devices and materials preparation

Research involving optimizing the efficiency and long-term stability of the perovskite materials is illustrated below. Four pieces of equipment are shown in Figure 8, where A is the reference equipment without any graphene materials; B has a graphene oxide inter-layer inserted between the perovskite active layers and the hole transport layers; C contains an electron transport layer with graphene doped into the TiO_2; D carries both the inter-layer and the "TiO_2-graphene" layer [24].

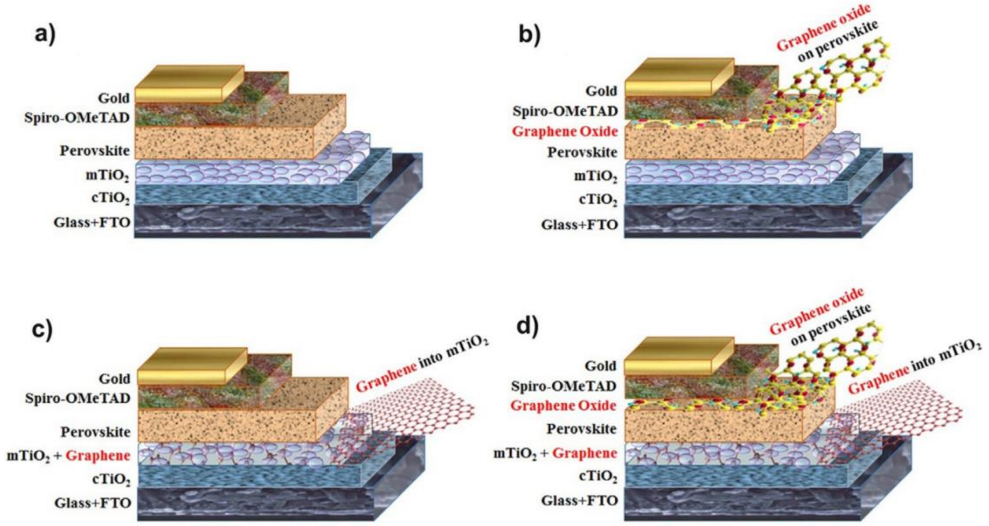

Figure 8. Different PSCs configurations [24].

4.3. *Methods*

The results evaluated by 1 sun are shown in Figure 9. The graphene oxide inter-layer and the doping of the graphene make little influence on the V_{OC}, while the inter-layers in devices B and C, respectively, make a significant contribution to the average J_{SC}; the device D, with both two layers, has demonstrated the best performances, whose efficiency has been over 18.2%, and significant improvements of the J_{SC} and fill factor concerning the reference PSC device can be observed as well [24].

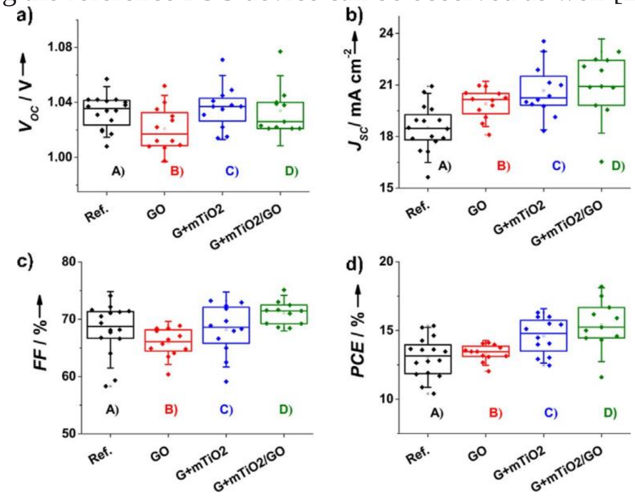

Figure 9. Efficiency tests for devices A–D [24].

The stability test of each device under exposure to prolonged light is reported in Figure 10, demonstrating that only device C has gained stronger stability than the reference device, with more than 88% of the initial PCE value after 16 h of the stress test. The filling factor of device C is always higher than that of the other three groups of devices, indicating that the solar cell of device C can still maintain relatively high output power under long-term operation, which to some extent makes up for the decomposition of perovskite material layer reflected in the figure of the normalized J_{sc} [24].

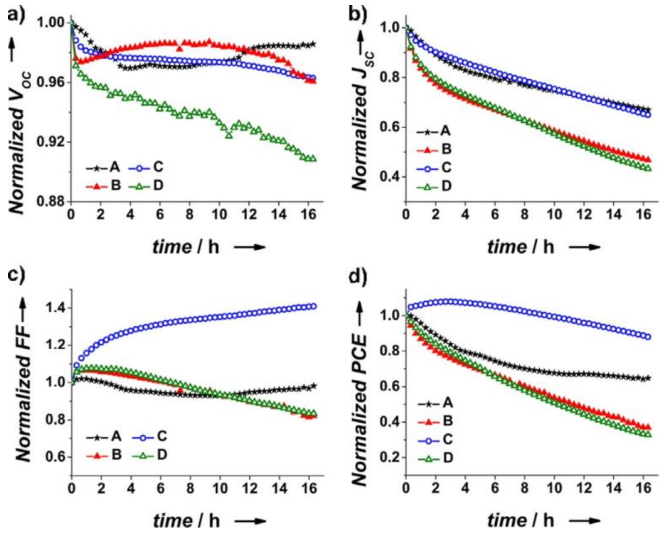

Figure 10. Normalized trends versus time under prolonged 1 sun illumination at MPP polarization provided by a calibrated white LED for devices A–D [24].

Overall, graphene materials and their derivatives have an impressive influence on the stability and efficiency of PSCs. PSCs with TiO_2-graphene interlayers have shown the best long-term performance [24]; the graphene oxide layer ameliorates the device's efficiency, while more consideration should be taken into the stability performance.

5. Conclusion

The development of PSCs has advanced significantly in a short amount of time. To compete with established photovoltaic technologies like silicon, cadmium telluride, and copper indium gallium selenide and sustain mass production, perovskite-based solar cells must first overcome many challenges. This paper describes the preparation process of perovskite and the failure principle. It lists three techniques for improving the stability and performance: perovskite materials' level, and the device lifetime under different stress conditions, including incorporating dye-sensitized solar cells (DSSC), doping, and graphene oxidation. According to the characteristics of different methods, this paper summarizes the common dyes used for dye sensitization, including coumarin, calixanthin, etc., and summarizes the principles and research progress of doping and graphene oxidation methods.

In this paper, it is believed that the future exploration of DSSCs can start from the preparation methods, such as: changing the ratio of precursor solution and the sintering temperature. Graphene, together with other 2D crystals or inorganic 2D crystals, acts as a dopant and an intermediate layer, which is important in improving the stability of perovskite-type solar cells. Interfacial engineering using graphene and related 2D materials (GRM) can be effectively used to improve the efficiency and regulate the stability of PSCs, which is also an idea to improve the stability of PCSs. In summary, perovskite solar materials offer a low-cost, high-efficiency option, but there is still room for further development of this technology due to its structural instability.

References

[1] Kojima A , Teshima K , Shirai Y 2019 *Journal of the American Chemical Society.* **131(17)** 6050-6051
[2] B. Chen, P.N. Rudd, S. Yang, Y. Yuan, J. Huang 2019 *Chem. Soc. Rev*. **48** 3842–3867
[3] M. Saliba, T. Matsui, K. Domanski, J.-Y. Seo, A. Ummadisingu, S.M. Zakeeruddin, J.-P. 2016 *Science.* **354** 206
[4] Sahli F, Werner J, Kamino BA, Bräuninger M, Monnard R, Paviet-Salomon B 2018 *Nat Mater* **17** 820–6
[5] Yinguo Zhou, Lei Zhang, Kai Zhou 2021 *Applied Surface Science.* Volume **543**, 148792, ISSN 0169-4332

[6] Shalini S, Balasundaraprabhu R, Kumar T S 2016 *International Journal of Energy Research.*
[7] F. Arkan, M. Izadyar 2019 *Appl. Phys. Lett.* **115** 183903
[8] D.-W. Kuo, G.-Z. Liu, R.-H. Lee 2019 *Dyes Pigments.* **17** 107562
[9] X. Feng, R. Chen, Z.-A.A. Nan, X. Lv, R. Meng, J. Cao, Y. Tang 2019 *Adv. Sci.* **6** 1802040
[10] Zhang S, Yang X, Numata Y et al. 2013 *Energy Environ Sci.* **6** 1443-1464
[11] Pastore M and Angelis FD 2010 *ACS Nano.* **4** 556-562
[12] Musleh, H., H. Zayed, S. Shaat, A. Al-Kahlout, H. Tamous, A. Issa, J. Asad and N. AlDahoudi 2019 *Egyptian Journal of Chemistry.* **62** 3-4
[13] Chen, Y., L. Zhang, J. Miao, J. Li 2020 *Dyes and Pigments.* **181**
[14] Zhao L N, Wang L, Hu X B 2011 *Chinese Journal of Materials Science and Engineering.* **29(6)** 811-815
[15] Qu D, Yao L F, Zhu Y A 2006 *Journal of University of Shanghai for Science and Technology.* **28(2)** 111-114
[16] Wang T W, Ball J M, Barea E M 2014 *Nano Letters.* **14(2)** 724
[17] Zhou H P, Chen Q, Li G 2014 *Science.* **345(6196)** 542
[18] Qin P, Domanski A L, Chandiran A K 2014 *Nanoscale* **6 (3)** 1508-1514.
[19] Zhang Q, Dandeneau C S, Zhou X 2009 *Advanced Materials.* **21(41)** 4087-4108.
[20] Han G Q, Wang S L, Chen X J 2008 *Journal of University of Shanghai for Science and Technology.* **30(6)** 573-577.
[21] Dong J, Zhao Y, Shi J 2014 *Chemical Communications.* **50(87)** 13381-13384
[22] Shirazi M, Dariani R S, Toroghinejad M R 2017 *Journal of Alloys &. Compounds.* **692** 492-502.
[23] Yin W, Yang J, Kang J 2015 *J. Mater. Chem. A* p 8926-8942
[24] Agresti A, Pescetelli S, Taheri B 2016 *ChemSusChem* **9(18)** 2609-2619
[25] Bonaccorso F, Colombo L, Yu G, Stoller M 2015 *Science* **347** 6217
[26] Feng S, Yang Y, Li M 2016 *ACS Appl. Mater. Interfaces* p 14503-14512